INFLUENCE OF MAGNETIC FIELD AND HEAT TRANSFER ON PERISTALTIC FLOW OF JEFFREY FLUID THROUGH A POROUS MEDIUM IN AN ASYMMETRIC CHANNEL

C. Vasudev[1], U. Rajeswara Rao[2], M. V. Subba Reddy[3] and G. Prabhakara Rao[2]
[1]Department of Science and Humanities, K.S. Institute of Technology, Bangalore, Karnataka, India
[2]Department of Mathematics, Sri Krishna Devaraya University, Anantapur, Andhra Pradesh, India
[3]Department of Information Technology, Sri Venkatesa Perumal College of Engineering and Technology, Puttur, India
E-Mail: raadha222@gmail.com

ABSTRACT

In this paper, we studied the effects of heat transfer and magnetic field on the peristaltic flow of a Jeffrey fluid through a porous medium in an asymmetric channel under the assumptions of long wavelength and low Reynolds number. Expressions for the velocity and pressure gradient are obtained analytically. The effects of Hartmann number, Darcy number, phase shift, Jeffrey fluid parameter and upper and lower wave amplitudes on the pumping characteristics and the temperature field are discussed through graphs in detail.

Keywords: darcy number, Hartmann number, heat transfer, Jeffrey fluid, phase shift, porous medium.

1. INTRODUCTION

During the last five decades researchers have extensively focused on the peristaltic flow of Newtonian fluids. Especially, peristaltic pumping occurs in many practical applications involving biomechanical systems such as roller and finger pumps. In particular, the peristaltic pumping of corrosive fluids and slurries could be useful as it is desirable to prevent their contact with mechanical parts of the pump. In these investigations, solutions for peristaltic flow of the fluid, the geometry of the channel and the propagating waves were obtained for various degrees of approximation.

Many researchers considered the fluid to behave like a Newtonian fluid for physiological peristalsis including the flow of blood in arterioles. But such a model cannot be suitable for blood flow unless the non - Newtonian nature of the fluid is included in it. Also the assumption that the chyme in small intestine is a Newtonian material of variable viscosity is not adequate in reality. Chyme is undoubtedly a non-Newtonian fluid. Provost and Schwarz [1] have explained a theoretical study of viscous effects in peristaltic pumping and assumed that the flow is free of inertial effects and that non-Newtonian normal stresses are negligible. Moreover, the Jeffrey model is relatively simpler linear model using time derivatives instead of convected derivatives for example the Oldroyd-B model does, it represents rheology different from the Newtonian. In spite of its relative simplicity, the Jeffrey model can indicate the changes of the rheology on the peristaltic flow even under the assumption of long wavelength, low Reynolds number and small or large amplitude ratio. Hayat *et al.* [2] investigated the effect of endoscope on the peristaltic flow of a Jeffrey fluid in a tube. Nagendra *et al.* [3] Peristaltic flow of a Jeffrey fluid in a tube. Furthermore, the MHD effect on peristaltic flow is important in technology (MHD pumps) and biology (blood flow). Such analysis is of great value in medical research. Mekheimer [4] studied the MHD peristaltic flow of a Newtonian fluid in a channel under the assumption of small wave number.

Therefore, at least in an initial study, this motivates an analytic study of MHD peristaltic non-Newtonian tube flow that holds for all non-Newtonian parameters. By choosing the Jeffrey fluid model it become possible to treat both the MHD Newtonian and non-Newtonian problems analytically under long wavelength and low Reynolds number considerations considering the blood as a MHD fluid, it may be possible to control blood pressure and its flow behavior by using an appropriate magnetic field. The influence of magnetic field may also be utilized as a blood pump for cardiac operations for blood flow in arterial stenosis or arteriosclerosis. Hayat and Ali [5] studied peristaltic flow of Jeffrey fluid under the effect of a magnetic field in tube. An effect of an endoscope and magnetic fluid on the peristaltic transport of a Jeffrey fluid was analyzed by Hayat *et al.* [6].

The investigations of blood flow through arteries are of considerable importance in many cardiovascular diseases particularly arteriosclerosis. In some pathological situations, the distribution of fatty cholesterol and artery clogging blood clots in the lumen of coronary artery can be considered as equivalent to a porous medium. El Shehaway and Husseny [7] and El Shehaway *et al.* [8] studied the peristaltic mechanism of a Newtonian fluid through a porous medium. Hayat *et al.* [9] investigated the MHD peristaltic flow of a porous medium in an asymmetric channel with heat transfer. Sudhakar Reddy *et al.* [10] studied the Peristaltic motion of a carreau fluid through a porous medium in a channel under the effect of a magnetic field.

Much attention had been confined to symmetric channels or tubes, but there exist also flows which may not be symmetric. Mishra and Rao [11] studied the peristaltic flow of a Newtonian fluid in an asymmetric channel in a recent research. In another attempt, Rao and Mishra [12] discussed the non-linear and curvature effects on peristaltic flow of a Newtonian fluid in an asymmetric

VOL. 5, NO. 12, DECEMBER 2010 ISSN 1819-6608
ARPN Journal of Engineering and Applied Sciences

www.arpnjournals.com

channel when the ratio of channel width to the wave length is small. An example for a peristaltic type motion is the intra-uterine fluid flow due to momentarily contraction, where the myometrial contractions may occur in both symmetric and asymmetric directions. An interesting study was made by Eytan and Elad [13] whose results have been used to analyze the fluid flow pattern in a non-pregnant uterus. In another paper, Eytan *et al*. [14] discussed the characterization of non-pregnant women uterine contractions as they are composed of variable amplitudes and a range of different wave lengths. Elshewey *et al*. [15] studied peristaltic flow of a Newtonian fluid through a porous medium in an asymmetric. Peristaltic transport of a power law fluid in an asymmetric channel was investigated by Subba Reddy *et al*. [16]. Ali and Hayat [17] discussed peristaltic flow of a Carreau fluid in an asymmetric channel.

The study of heat transfer analysis is another important area in connection with peristaltic motion, which has industrial applications like sanitary fluid transport, blood pumps in heart lungs machine and transport of corrosive fluids where the contact of fluid with the machinery parts are prohibited. There are only a limited number of research available in literature in which peristaltic phenomenon has discussed in the presence of heat transfer (Mekheimer, Elmaboud, [18]; Vajravelu *et al*., [19]; Radhakrishnamacharya, Srinivasulu, [20]; Srinivas, Kothandapani, [21]).

However, the influence of magnetic field with peristaltic flow of a Jeffrey fluid through a porous medium in an asymmetric channel has received little attention. Hence, an attempt is made to study the MHD peristaltic flow of a Jeffrey fluid through a porous medium in an asymmetric channel under the assumptions of long wavelength and low Reynolds number. Expressions for the velocity and pressure gradient are obtained analytically. The effects of Hartmann number M , Darcy number Da, phase shift θ, Jeffrey fluid parameter λ_1 and wave amplitudes ϕ_1 and ϕ_2 on the pumping characteristics are studied in detail.

2. MATHEMATICAL FORMULATION

We consider the flow of an incompressible electrically conducting Jeffrey fluid through a porous medium in a two-dimensional asymmetric channel induced by sinusoidal wave trains propagating with constant speed c along the channel walls. A rectangular co-ordinate system (X, Y) is chosen such that X-axis lies along the centre line of the channel in the direction of wave propagation and Y-axis transverse to it, as shown in Figure-1.

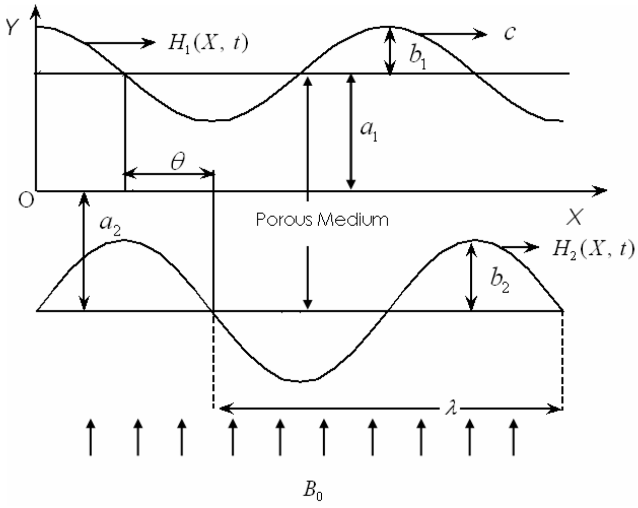

Figure-1. The physical model.

The channel walls are characterized by

$$Y = H_1(X,t) = a_1 + b_1\cos\frac{2\pi}{\lambda}(X - ct) \quad \text{(Upper wall) (2.1a)}$$

$$Y = H_2(X,t) = -a_2 - b_2\cos\left(\frac{2\pi}{\lambda}(X - ct) + \theta\right) \quad \text{(Lower wall)(2.1b)}$$

where b_1, b_2 are the amplitudes of the waves, λ is the wavelength, $a_1 + a_2$ is the width of the channel, θ is the phase difference which varies in the range $0 \le \theta \le \pi$, $\theta = 0$ corresponds to a symmetric channel with waves out of phase and $\theta = \pi$ defines the waves with in phase and further a_1, a_2, b_1, b_2 and θ satisfies the condition $b_1^2 + b_2^2 + 2b_1b_2\cos\theta \le (a_1 + a_2)^2$.

A uniform magnetic field B_0 is applied in the transverse direction to the flow. The electrical conductivity of the fluid is assumed to be small so that the magnetic Reynolds number is small and the induced magnetic field is neglected in comparison with the applied magnetic field. The external electric field is zero and the electric field due to polarization of charges is also negligible. Heat due to Joule dissipation is neglected.

In fixed frame (X,Y), the flow is unsteady but if we choose moving frame (x, y), which travel in the *X*-direction with the same speed as the peristaltic wave, then the flow can be treated as steady.

The transformation between two frames are related by

$$x = X - ct,\ y = Y,\ u = U - c,\ v = V \text{ and } p(x) = P(X,t) \quad (2.2)$$

Where (u,v) and (U,V) are the velocity components, p and P are the pressures in wave and fixed frames of reference respectively.

The pressure p remains a constant across any axial station of the channel, under the assumption that the

VOL. 5, NO. 12, DECEMBER 2010 ISSN 1819-6608
ARPN Journal of Engineering and Applied Sciences

www.arpnjournals.com

wavelength is large and the curvature effects are negligible.

The constitutive equation for stress tensor τ in Jeffrey fluid is

$$\tau = \frac{\mu}{1+\lambda_1}(\dot{\gamma} + \lambda_2 \ddot{\gamma}) \tag{2.3}$$

Where λ_1 the ratio of relaxation time to retardation time is' λ_2 is the retardation time, μ - the dynamic viscosity, $\dot{\gamma}$ - the shear rate and dots over the quantities indicate differentiation with respect to time t.

In the absence of an input electric field, the equations governing the flow field in a wave frame are

$$\frac{\partial u}{\partial x} + \frac{\partial v}{\partial y} = 0 \tag{2.4}$$

$$\rho\left(u\frac{\partial u}{\partial x} + v\frac{\partial u}{\partial y}\right) = -\frac{\partial p}{\partial x} + \frac{\partial \tau_{xx}}{\partial x} + \frac{\partial \tau_{xy}}{\partial y} - \frac{\mu}{k_0}(u+c) - \sigma B_0^2(u+c) \tag{2.5}$$

$$\rho\left(u\frac{\partial v}{\partial x} + v\frac{\partial v}{\partial y}\right) = -\frac{\partial p}{\partial x} + \frac{\partial \tau_{yx}}{\partial x} + \frac{\partial \tau_{yy}}{\partial y} - \frac{\mu}{k}v \tag{2.6}$$

$$\zeta\left[u\frac{\partial T}{\partial x} + v\frac{\partial T}{\partial y}\right] = \frac{k}{\rho}\nabla^2 T + \nu\left\{2\left[\left(\frac{\partial u}{\partial x}\right)^2 + \left(\frac{\partial v}{\partial y}\right)^2\right] + \left(\frac{\partial u}{\partial y} + \frac{\partial v}{\partial x}\right)^2\right\} \tag{2.7}$$

where ρ is the density, μ is the co-efficient of viscosity of the fluid, k_0 is the permeability of the porous medium, σ is the electrical conductivity of the fluid, ζ is the specific heat at constant volume, ν is kinematic viscosity of the fluid, k is thermal conductivity of the fluid and T is temperature of the fluid and B_0 -magnetic field strength.

In order to write the governing equations and the boundary conditions in dimensionless form the following non - dimensional quantities are introduced.

$$\bar{x} = \frac{x}{\lambda}; \bar{y} = \frac{y}{a_1}; \bar{u} = \frac{U}{c}, \bar{v} = \frac{V}{c\delta}, \delta = \frac{d}{\lambda}, \bar{p} = \frac{a_1^2 p}{\mu c \lambda}, \bar{t} = \frac{ct}{\lambda}, h_1 = \frac{H_1}{a_1}, d = \frac{a_2}{a_1},$$

$$h_2 = \frac{H_2}{a_1}, \phi_1 = \frac{b_1}{a_1}, \phi_2 = \frac{b_2}{a_1}, \Theta = \frac{T-T_0}{T_1-T_0}, \Pr = \frac{\rho\nu\zeta}{k}, E = \frac{c^2}{\zeta(T_1-T_0)} \tag{2.8}$$

Where δ is the wave number and ϕ_1 and ϕ_2 are amplitude ratios.

In view of (2.8), the Equations (2.4) - (2.7), after dropping bars, reduce to

$$\frac{\partial u}{\partial x} + \frac{\partial v}{\partial y} = 0 \tag{2.9}$$

$$\mathrm{Re}\,\delta\left(u\frac{\partial u}{\partial x} + v\frac{\partial u}{\partial y}\right) = -\frac{\partial p}{\partial x} + \frac{\partial \tau_{xx}}{\partial x} + \delta\frac{\partial \tau_{xy}}{\partial y} - \left[\frac{1}{Da} + M^2\right](u+1) \tag{2.10}$$

$$\mathrm{Re}\,\delta^3\left(u\frac{\partial v}{\partial x} + v\frac{\partial v}{\partial y}\right) = -\frac{\partial p}{\partial x} + \delta^2\frac{\partial \tau_{yx}}{\partial x} + \delta\frac{\partial \tau_{yy}}{\partial y} - \frac{\delta^2}{Da}v \tag{2.11}$$

$$\mathrm{Re}\,\delta\left[u\frac{\partial \Theta}{\partial x} + v\frac{\partial \Theta}{\partial y}\right] = \frac{1}{\Pr}\left(\delta^2\frac{\partial^2\Theta}{\partial x^2} + \frac{\partial^2\Theta}{\partial y^2}\right)$$

$$+E\left\{4\delta^2\left(\frac{\partial u}{\partial x}\right)^2 + \left(\frac{\partial u}{\partial y}\right)^2 + \delta^4\left(\frac{\partial v}{\partial x}\right)^2 + 2\delta^2\frac{\partial u}{\partial y}\frac{\partial v}{\partial x}\right\} \tag{2.12}$$

Where $\mathrm{Re} = \frac{\rho a_1 c}{\mu}$ is the Reynolds number, $M^2 = \frac{\sigma a_1^2 B_0^2}{\mu}$ is the Hartmann number.

Also $\tau_{xx} = \delta\frac{2}{(1+\lambda_1)}\left[1 + \frac{\lambda_2 c\delta}{a_1}\left(u\frac{\partial}{\partial x} + v\frac{\partial}{\partial y}\right)\right]\frac{\partial u}{\partial x}$,

$$\tau_{xy} = \frac{1}{(1+\lambda_1)}\left[1 + \frac{\lambda_2 c\delta}{a_1}\left(u\frac{\partial}{\partial x} + v\frac{\partial}{\partial y}\right)\right]\left(\frac{\partial u}{\partial y} + \delta^2\frac{\partial v}{\partial x}\right),$$

$$\tau_{yy} = \frac{2\delta}{(1+\lambda_1)}\left[1 + \frac{\lambda_2 c\delta}{a_1}\left(u\frac{\partial}{\partial x} + v\frac{\partial}{\partial y}\right)\right]\frac{\partial v}{\partial y}.$$

Under the assumptions of long wave length $(\delta << 1)$ and low Reynolds number $(\mathrm{Re} \to 0)$, the Equations (2.10) - (2.12) become

$$\frac{\partial p}{\partial x} = \frac{1}{1+\lambda_1}\frac{\partial^2 u}{\partial y^2} - \left[\frac{1}{Da} + M^2\right](u+1) \tag{2.13}$$

$$\frac{\partial p}{\partial y} = 0 \tag{2.14}$$

VOL. 5, NO. 12, DECEMBER 2010 ISSN 1819-6608
ARPN Journal of Engineering and Applied Sciences

www.arpnjournals.com

$$\frac{1}{Pr}\left[\frac{\partial^2\Theta}{\partial y^2}\right]+E\left[\frac{\partial u}{\partial y}\right]^2=0 \tag{2.15}$$

The non-dimensional boundary conditions are

$$u=-1 \text{ at } y=h_1,h_2 \tag{2.16}$$

$$\Theta=0 \text{ at } y=h_1\left(x\right) \tag{2.17}$$

$$\Theta=1 \text{ at } y=h_2\left(x\right) \tag{2.18}$$

Equation (2.14) implies that $p \neq p(y)$, hence p is only function of x.
Therefore, the Equation (2.13) can be rewritten as

$$\frac{dp}{dx}=\frac{1}{1+\lambda_1}\frac{\partial^2 u}{\partial y^2}-\left[\frac{1}{Da}+M^2\right]\left(u+1\right) \tag{2.19}$$

The rate of volume flow rate through each section in a wave frame, is calculated as

$$q=\int_{h_2}^{h_1}udy \tag{2.20}$$

The flux at any axial station in the laboratory frame is

$$Q\left(x,t\right)=\int_{h_2}^{h_1}\left(u+1\right)dy=q+h_1-h_2 \tag{2.21}$$

The average volume flow rate over one period ($T=\lambda/c$) of the peristaltic wave is defined as

$$\overline{Q}=\frac{1}{T}\int_0^T Q\,dt=q+1+d \tag{2.22}$$

The dimensionless pressure rise per one wavelength in the wave frame is defined as

$$\Delta p=\int_0^1\frac{dp}{dx}dx \tag{2.23}$$

3. SOLUTION OF THE PROBLEM

Solving Equation (2.19) using boundary conditions (2.16), we get

$$u=\left(\frac{1+\lambda_1}{N^2}\right)\frac{dp}{dx}\left[c_1\cosh Ny+c_2\sinh Ny-1\right]-1 \tag{3.1}$$

Where $N^2=\left(1+\lambda_1\right)\left[\frac{1}{Da}+M^2\right]$, $c_1=\frac{\sinh Nh_2-\sinh Nh_1}{\sinh N(h_2-h_1)}$

and $c_2=\frac{\cosh Nh_1-\cosh Nh_2}{\sinh N(h_2-h_1)}$.

Substituting Equation (3.1) in the Equation (2.15) and Solving Equation (2.15) using the boundary conditions (2.17) and (2.18), we obtain

$$\Theta=c_3+c_4y-E\Pr\frac{\left(1+\lambda_1\right)^2}{\left(8N^4\right)}\left(\frac{dp}{dx}\right)^2\left[\begin{array}{l}\left(c_1^2+c_2^2\right)\cosh 2Ny+2c_1c_2\sinh 2Ny\\+2\left(c_2^2-c_1^2\right)y^2\end{array}\right] \tag{3.2}$$

Where $c_3=-c_4h_1+\frac{E\Pr c_5}{8N^4}\left(1+\lambda_1\right)^2\left(\frac{dp}{dx}\right)^2$,

$c_4=\frac{1}{h_2-h_1}+\frac{E\Pr\left(c_6-c_5\right)\left(1+\lambda_1\right)^2}{8\left(h_2-h_1\right)N^4}\left(\frac{dp}{dx}\right)^2$,

$c_5=\left(c_1^2+c_2^2\right)\cosh 2Nh_1+2c_1c_2\sinh 2Nh_1+2\left(c_2^2-c_1^2\right)h_1^2$,

and

$c_6=\left(c_1^2+c_2^2\right)\cosh 2Nh_2+2c_1c_2\sinh 2Nh_2+2\left(c_2^2-c_1^2\right)h_2^2$.

The volume flow rate q in the wave frame of reference is given by

$$q=\frac{\left(1+\lambda_1\right)}{N^3}\frac{dp}{dx}\frac{\left[2-2\cosh N\left(h_1-h_2\right)-N\left(h_1-h_2\right)\sinh N\left(h_2-h_1\right)\right]}{\sinh N(h_2-h_1)}$$

$$-\left(h_1-h_2\right) \tag{3.3}$$

From (3.3), we have

$$\frac{dp}{dx}=\frac{N^3}{\left(1+\lambda_1\right)}\frac{\left(q+h_1-h_2\right)\sinh N(h_2-h_1)}{\left[2-2\cosh N(h_1-h_2)-N(h_1-h_2)\sinh N(h_2-h_1)\right]} \tag{3.4}$$

The heat transfer coefficient at the upper wall is defined by

$$Z=\frac{\partial\Theta}{\partial y}\frac{\partial h_1}{\partial x}\bigg|_{y=h_1}=-2\pi\phi_1\sin 2\pi x\left[c_4-\frac{\Pr E\left(1+\lambda_1\right)^2}{8N^4}\left(\frac{dp}{dx}\right)^2c_7\right]$$

Where

$$c_7 = 2N\left(c_1^2 + c_2^2\right)\sinh 2Nh_1 + 4c_1c_2N\cosh 2Nh_1 + 4\left(c_2^2 - c_1^2\right)h_1$$

4. RESULTS AND DISCUSSIONS

In order to get the physical insight of the problem, pumping characteristics and temperature field are computed numerically for different values of various emerging parameters, viz., phase shift θ, Darcy number Da, Hartmann number M, amplitude ratios ϕ_1, ϕ_2, channel width d and Jeffrey fluid parameter λ_1 and are presented in Figures 2-16.

The variation of pressure rise Δp with time averaged flux $\overline{Q}$ for different values of phase shift θ with $\phi_1 = 0.6$, $\phi_2 = 0.9$, $\lambda_1 = 0.3$, $M = 1$, $Da = 0.1$ and $d = 2$ is depicted in Figure-2. It is found that, the $\overline{Q}$ decreases with increasing phase shift θ in all the three regions, viz., pumping region $(\Delta p > 0)$, free pumping region $(\Delta p = 0)$ and co-pumping region $(\Delta p < 0)$. Moreover, the $\overline{Q}$ increases with increasing θ for appropriately chosen $\Delta p(< 0)$.

Figure-3 shows the variation of pressure rise Δp with time averaged flux $\overline{Q}$ for different values of Hartmann number M with $\phi_1 = 0.6$, $\phi_2 = 0.9$, $\lambda_1 = 0.3$, $\theta = \frac{\pi}{4}$, $Da = 0.1$ and $d = 2$. It is observed that, any two pumping curves intersect in first quadrant to the left of this point of intersection the $\overline{Q}$ increases with increasing M and to the right side of this point of intersection the $\overline{Q}$ decreases with increasing M.

The variation of pressure rise Δp with $\overline{Q}$ for different values of Darcy number Da with $\phi_1 = 0.6$, $\phi_2 = 0.9$, $\lambda_1 = 0.3$, $M = 1$, $\theta = \frac{\pi}{4}$ and $d = 2$ is presented in Figure-4. It is noted that, in the pumping region $(\Delta p > 0)$, the $\overline{Q}$ decreases with increasing Da whereas it increases with Da in both free pumping $(\Delta p = 0)$ and co-pumping $(\Delta p < 0)$ regions.

Figure-5 depicts the variation of pressure rise Δp with time averaged flux $\overline{Q}$ for different values of λ_1 with $\phi_1 = 0.6, \phi_2 = 0.9$ $Da = 0.1$, $\theta = \frac{\pi}{4}$, $M = 1$ and $d = 2$. It is observed that, the $\overline{Q}$ decreases with increases λ_1 in both the pumping and free pumping regions, while in the co-pumping region, the $\overline{Q}$ increases with increasing λ_1.

The variation of pressure rise Δp with time averaged flux $\overline{Q}$ for different values of ϕ_1 with $\phi_2 = 0.9, \lambda_1 = 0.3,$ $Da = 0.1$, $\theta = \frac{\pi}{4}$, $M = 1$ and $d = 2$ is shown in Figure-6. It is found that, the $\overline{Q}$ increases with an increase in ϕ_1 in both pumping and free pumping regions. But in the co-pumping region, the $\overline{Q}$ decreases with increasing ϕ_1, for an appropriately chosen $\Delta p(< 0)$.

Figure-7 represents the variation of pressure rise Δp with time averaged flux $\overline{Q}$ for different values of ϕ_2 with $\phi_1 = 0.6, \lambda_1 = 0.3,$ $Da = 0.1$, $\theta = \frac{\pi}{4}$, $M = 1$ and $d = 2$. It is noted that, as ϕ_2 increases, the $\overline{Q}$ increases in both pumping and free pumping regions, while in co-pumping region, the $\overline{Q}$ decreases as ϕ_2 increases, for an appropriately chosen $\Delta p(< 0)$.

Figure-8 shows the variation of pressure rise Δp with time averaged flux $\overline{Q}$ for different values of d with $\phi_1 = 0.6, \phi_2 = 0.9,$ $Da = 0.1$, $\theta = \frac{\pi}{4}$, $M = 1$ and $\lambda_1 = 0.3$. It is noted that, as d increases, the $\overline{Q}$ decreases in both pumping and free pumping regions, but in co-pumping region, the $\overline{Q}$ increases as d increases, for an appropriately chosen $\Delta p(< 0)$.

Figure-9 shows the temperature profiles for different values of phase shift θ with $\phi_1 = 0.6, \phi_2 = 0.9, q = -1, M = 1, x = 0.2$, $Da = 0.1$, $\lambda_1 = 0.3, d = 2$ and $PrE = 2$. It is found that, as increasing in θ decreases the amplitude of the temperature at the inlet.

Effect of Hartmann number M on the temperature field for different for $\phi_1 = 0.6$, $\phi_2 = 0.9$,

ARPN Journal of Engineering and Applied Sciences

$q=-1, \theta=\frac{\pi}{4}, x=0.2, Da=0.1, \lambda_1=0.3, d=2$ and $PrE=2$ is shown in Figure-10. It is observed that, the temperature profiles are all most parabolic and temperature Θ decreases with increasing M.

Figure-11 depicts the temperature profiles for different values of Hartmann number M with $\phi_1=0.6, \phi_2=0.9, q=-1, \theta=\frac{\pi}{4}, x=0.2, Da=0.1$, $\lambda_1=0.3, d=2$ and $PrE=2$. It is found that, the temperature Θ decreases with increasing M.

Effect of Darcy number Da on the temperature profiles for $\phi_1=0.6, \phi_2=0.9, q=-1, \theta=\frac{\pi}{4}, x=0.2, M=1$, $\lambda_1=0.3, d=2$ and $PrE=2$ is presented in Figure-12. It is observed that, the Θ increases with increasing Da.

Figure-13 represents the temperature profiles for different values of λ_1 with $\phi_1=0.6, \phi_2=0.9, \theta=\frac{\pi}{4}$, $x=0.2, Da=0.1, q=-1, M=1, d=2$ and $PrE=2$. It is noted that, the Θ decreases with an increase λ_1.

Temperature profiles for different values of ϕ_1 with $\lambda_1=0.3, \phi_2=0.9, q=-1, \theta=\frac{\pi}{4}$, $x=0.2, Da=0.1, M=1, d=2$ and $PrE=2$ is shown in Figure-14. It is observed that, the temperature Θ increases with an increase in ϕ_1

Figure-15 depicts the temperature profiles for different values of ϕ_2 with $\phi_1=0.6, \theta=\frac{\pi}{4}$, $\lambda_1=0.3, q=-1, x=0.2, Da=0.1, M=1, d=2$ and $PrE=2$. It is found that, the temperature Θ increases with an increase in ϕ_2. Further it is observed that the significant variation in Θ occurs only near the lower wall.

Temperature profiles for different values of d with $\phi_1=0.6, \phi_2=0.9$, $q=-1, \theta=\frac{\pi}{4}, x=0.2, Da=0.1, M=1, \lambda_1=0.3$ and $PrE=2$ is presented in Figure-16. It is noted that, the temperature Θ decreases with an increase in ϕ_2.

Figure-17. Temperature profiles for different values of $\Pr E$ with $\phi_1=0.6, \phi_2=0.9, q=-1, \theta=\frac{\pi}{4}$, $x=0.2, Da=0.1, M=1, \lambda_1=0.3$ and $d=2$. It is observed that, the temperature Θ increases with an increase in $\Pr E$.

In order to see the effects of $\theta, \Pr E, M, Da$ and ϕ_1 on the heat transfer coefficient Z at the upper wall we have compute numerically and are presented in Tables 1-5. Table-1 shows that, the heat transfer coefficient Z increases with increasing phase shift θ. From Table-2, we found that the heat transfer coefficient Z increases with an increase in $\Pr E$. Table-3 shows that, the heat transfer coefficient Z increases with increasing M. From Table-4, we noted that the heat transfer coefficient Z decreases with increasing Da. From Table-5, we conclude that heat transfer coefficient Z increases with increasing ϕ_1

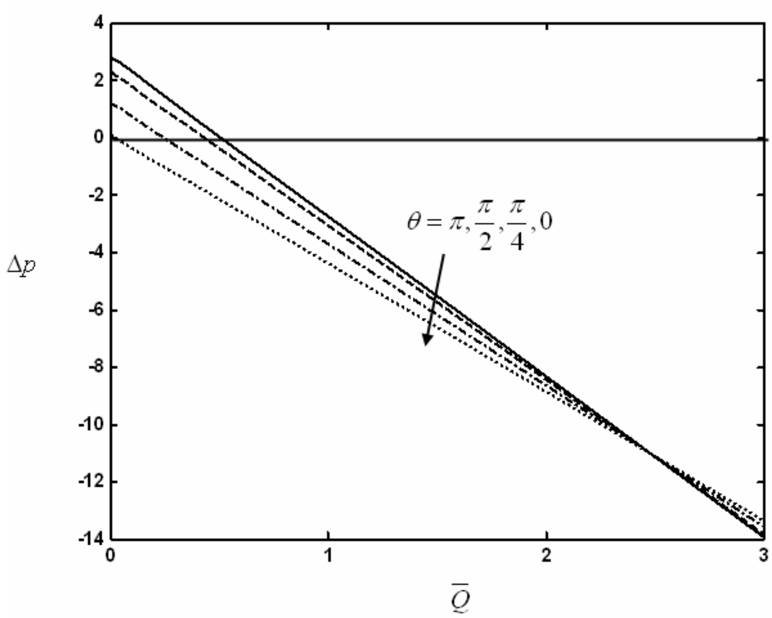

Figure-2. The variation of pressure rise Δp with $\overline{Q}$ for different values of phase shift θ with $\phi_1 = 0.6, \phi_2 = 0.9$, $\lambda_1 = 0.3$, $M = 1, Da = 0.1$ and $d = 2$.

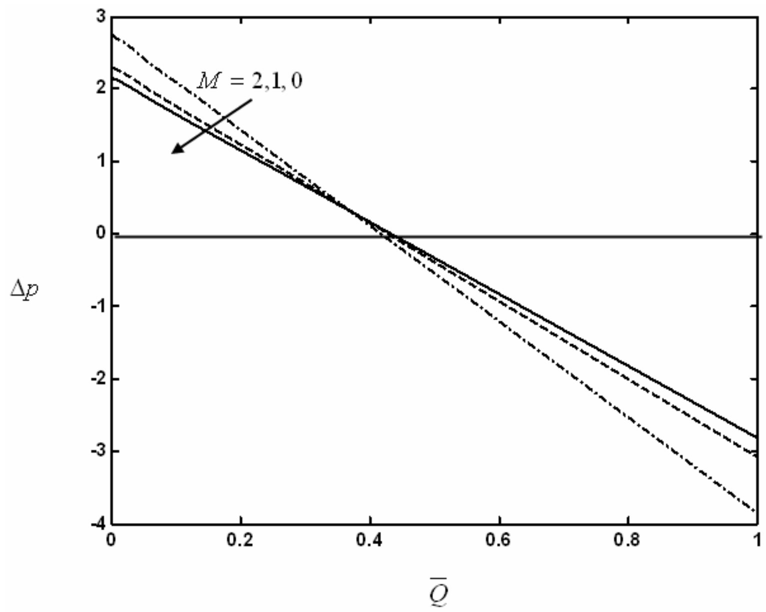

Figure-3. The variation of pressure rise Δp with $\overline{Q}$ for different values of Hartmann number M with $\phi_1 = 0.6, \phi_2 = 0.9$

$$\lambda_1 = 0.3, \theta = \frac{\pi}{4}, Da = 0.1 \text{ and } d = 2.$$

VOL. 5, NO. 12, DECEMBER 2010 ISSN 1819-6608
ARPN Journal of Engineering and Applied Sciences

www.arpnjournals.com

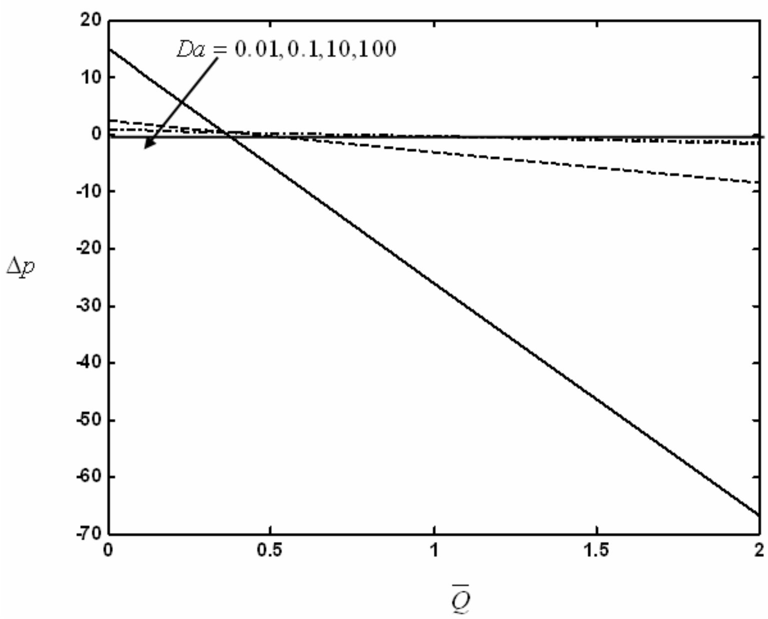

Figure-4. The variation of pressure rise Δp with $\overline{Q}$ for different values of Darcy number Da with $\phi_1 = 0.6, \phi_2 = 0.9$ $\lambda_1 = 0.3, \theta = \dfrac{\pi}{4}, M = 1$ and $d = 2$.

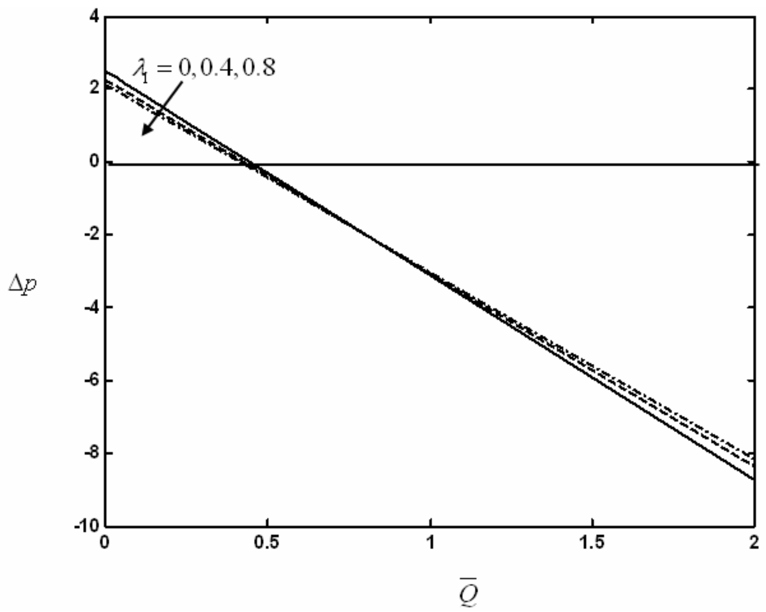

Figure-5. The variation of pressure rise Δp with $\overline{Q}$ for different values of λ_1 with $\phi_1 = 0.6, \phi_2 = 0.9$ $Da = 0.1$, $\theta = \dfrac{\pi}{4}$, $M = 1$ and $d = 2$.

ARPN Journal of Engineering and Applied Sciences

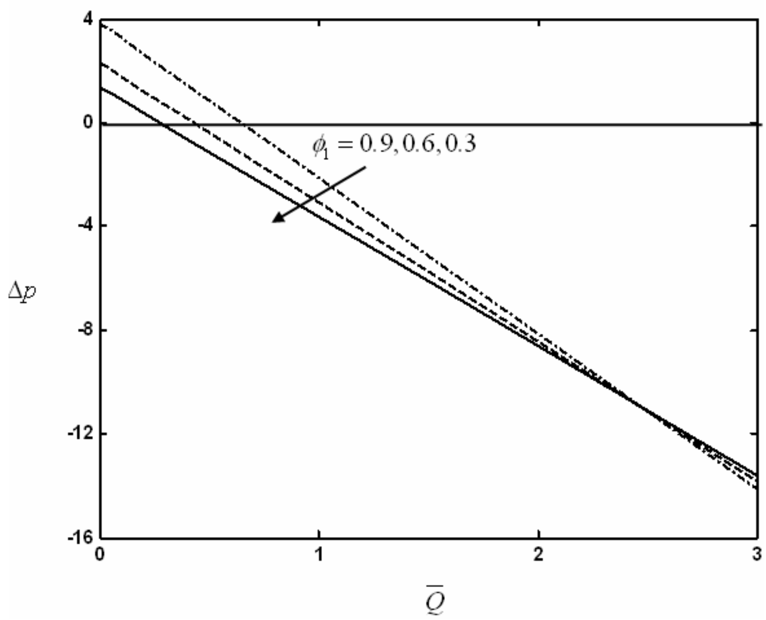

Figure-6. The variation of pressure rise Δp with $\overline{Q}$ for different values of ϕ_1 with $\phi_2 = 0.9, \lambda_1 = 0.3,\ Da = 0.1,\ \theta = \frac{\pi}{4},$ $M = 1$ and $d = 2$.

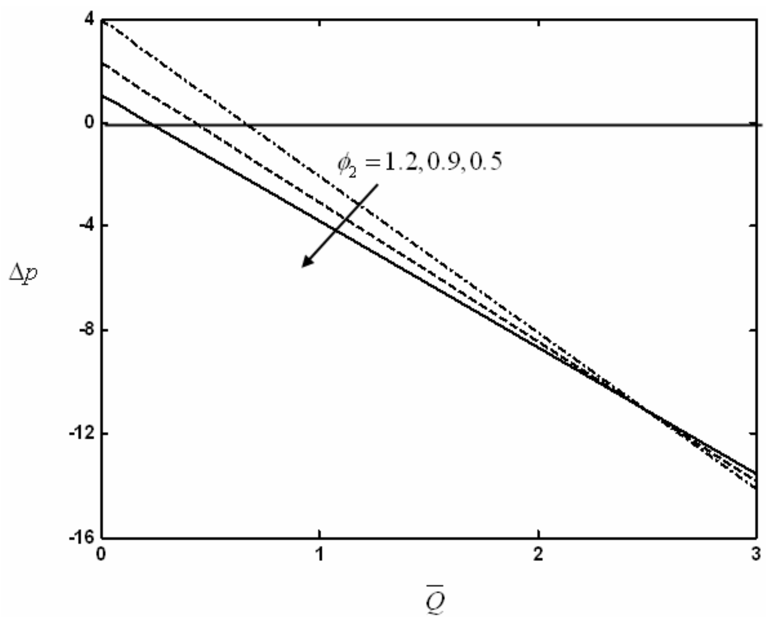

Figure-7. The variation of pressure rise Δp with $\overline{Q}$ for different values of ϕ_2 with $\phi_1 = 0.6, \lambda_1 = 0.3,\ Da = 0.1,\ \theta = \frac{\pi}{4},$ $M = 1$ and $d = 2$.

ARPN Journal of Engineering and Applied Sciences

www.arpnjournals.com

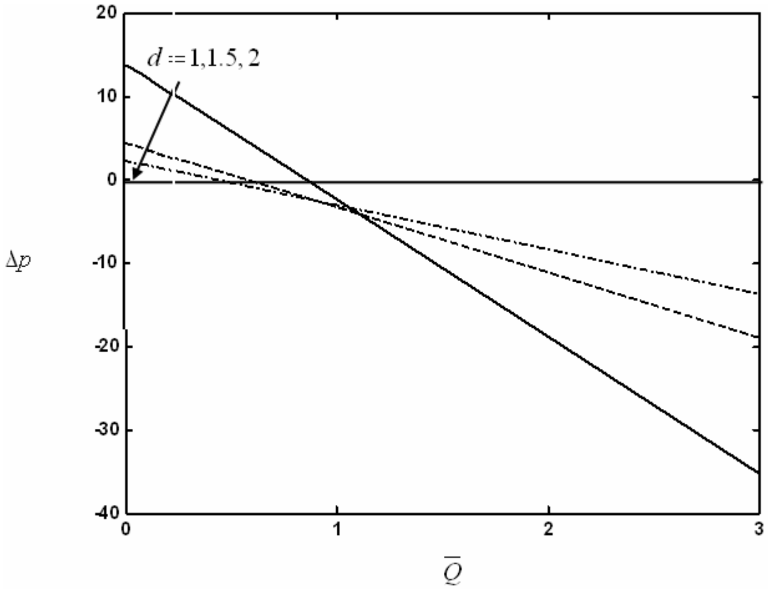

Figure-8. The variation of pressure rise Δp with $\overline{Q}$ for different values of d with $\phi_1 = 0.6, \phi_2 = 0.9,\ Da = 0.1$, $\theta = \frac{\pi}{4}$, $M = 1$ and $\lambda_1 = 0.3$.

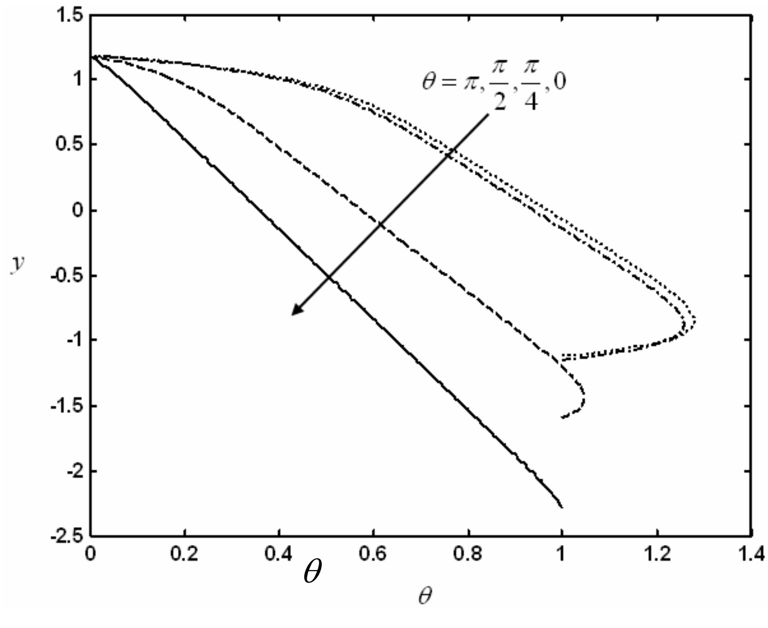

Figure-9. Temperature profiles for different values of phase shift θ with $\phi_1 = 0.6, \phi_2 = 0.9, q = -1, M = 1, x = 0.2$, $Da = 0.1$, $\lambda_1 = 0.3, d = 2$ and $\Pr E = 2$.

ARPN Journal of Engineering and Applied Sciences

www.arpnjournals.com

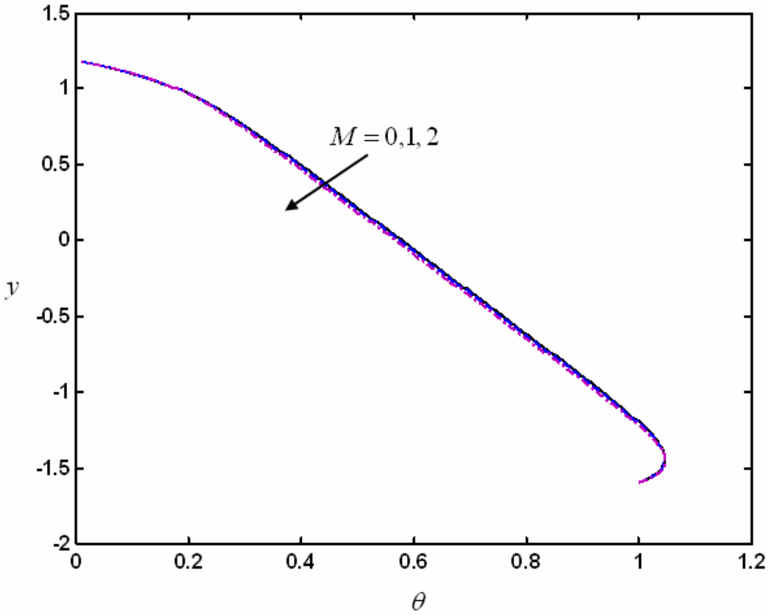

Figure-10. Temperature profiles for different values of hartmann number M with $\phi_1 = 0.6, \phi_2 = 0.9, q = -1, \theta = \frac{\pi}{4}$, $x = 0.2$, $Da = 0.1$, $\lambda_1 = 0.3, d = 2$ and $\Pr E = 2$.

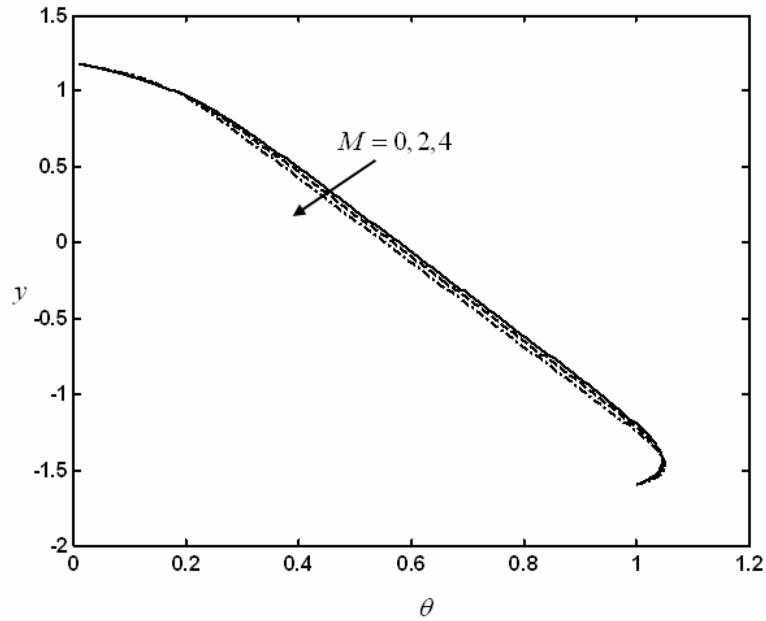

Figure-11. Temperature profiles for different values of hartmann number M with $\phi_1 = 0.6, \phi_2 = 0.9, q = -1, \theta = \frac{\pi}{4}$, $x = 0.2$, $Da = 0.1$, $\lambda_1 = 0.3, d = 2$ and $\Pr E = 2$.

VOL. 5, NO. 12, DECEMBER 2010 ISSN 1819-6608
ARPN Journal of Engineering and Applied Sciences

www.arpnjournals.com

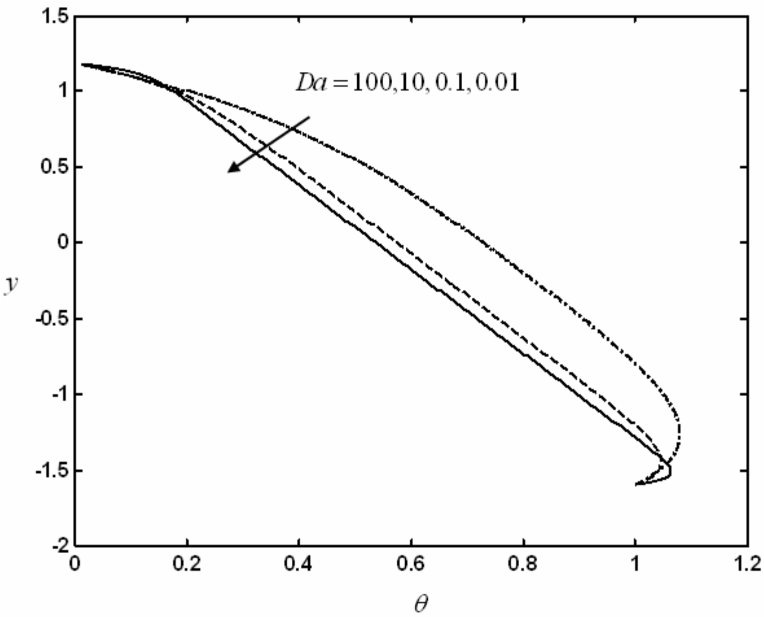

Figure-12. Temperature profiles for different values of darcy number Da with $\phi_1 = 0.6, \phi_2 = 0.9, q = -1,\ \theta = \frac{\pi}{4}$, $x = 0.2$, $M = 1, \lambda_1 = 0.3, d = 2$ and $\Pr E = 2$.

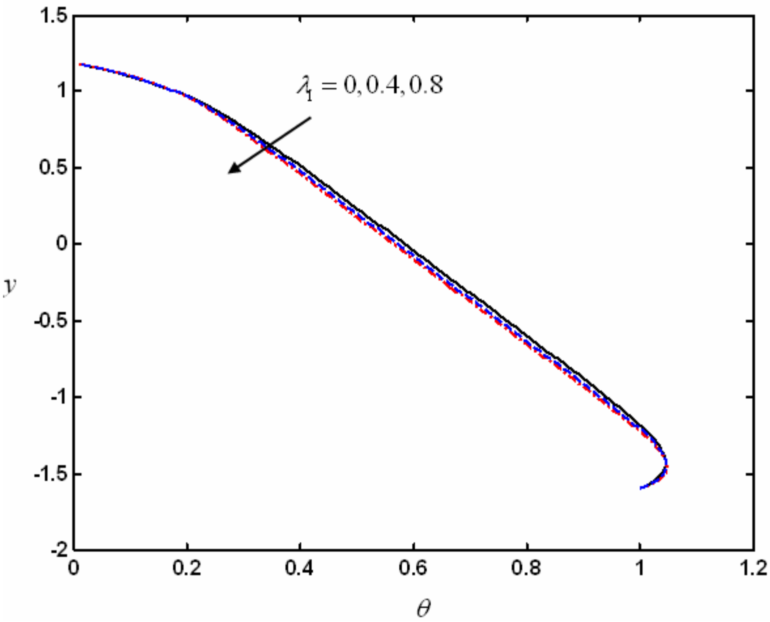

Figure-13. Temperature profiles for different values of λ_1 with $\phi_1 = 0.6, \phi_2 = 0.9, q = -1,\ \theta = \frac{\pi}{4},\ x = 0.2, Da = 0.1$, $M = 1, d = 2$ and $\Pr E = 2$.

VOL. 5, NO. 12, DECEMBER 2010 ISSN 1819-6608
ARPN Journal of Engineering and Applied Sciences

www.arpnjournals.com

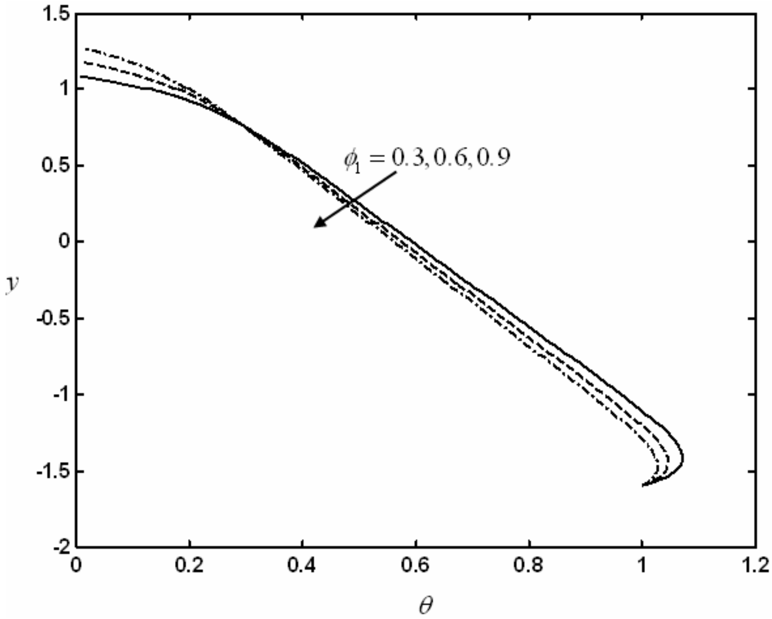

Figure-14. Temperature profiles for different values of ϕ_1 with

$$\lambda_1 = 0.3, \phi_2 = 0.9, q = -1,\ \theta = \frac{\pi}{4},\ x = 0.2, Da = 0.1,$$
$$M = 1, d = 2 \text{ and } \Pr E = 2.$$

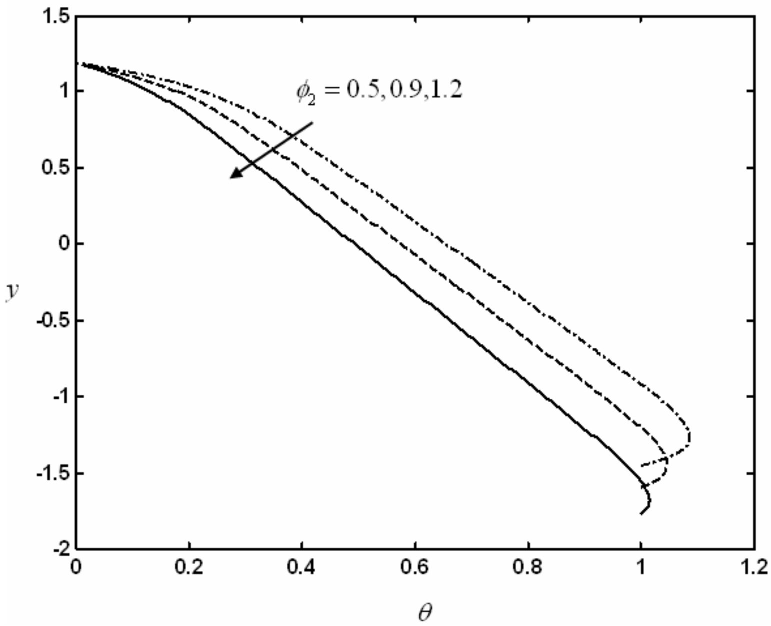

Figure-15. Temperature profiles for different values of ϕ_2 with

$$\phi_1 = 0.6, \lambda_1 = 0.3, q = -1,\ \theta = \frac{\pi}{4},\ x = 0.2, Da = 0.1,$$
$$M = 1, d = 2 \text{ and } \Pr E = 2.$$

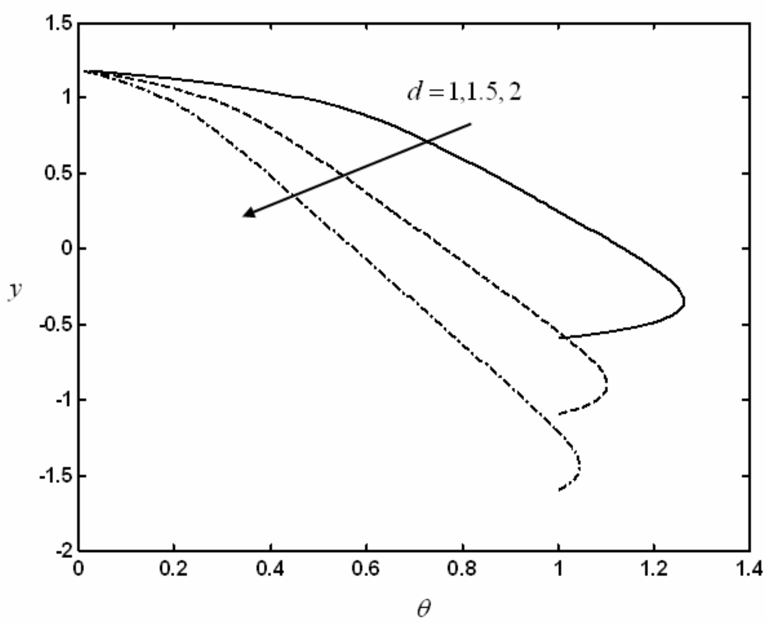

Figure-16. Temperature profiles for different values of d with

$\phi_1 = 0.6, \phi_2 = 0.9, q = -1,\ \theta = \dfrac{\pi}{4},\ x = 0.2, Da = 0.1,$
$M = 1, \lambda_1 = 0.3$ and $\Pr E = 2$.

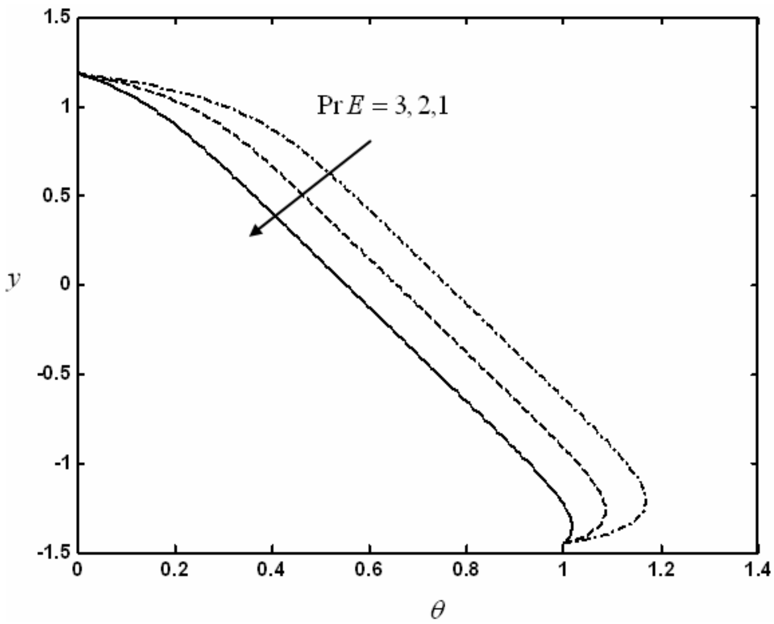

Figure-17. Temperature profiles for different values of $\Pr E$ with

$\phi_1 = 0.6, \phi_2 = 0.9, q = -1,\ \theta = \dfrac{\pi}{4},\ x = 0.2, Da = 0.1,$
$M = 1, \lambda_1 = 0.3$ and $d = 2$.

ARPN Journal of Engineering and Applied Sciences

www.arpnjournals.com

Table-1. The variation of heat transfer coefficient Z with θ for $\phi_1 = 0.6$, $\phi_2 = 0.9$, $\lambda_1 = 0.3$, $M = 1, Da = 0.1, \Pr E = 2$ and $d = 2$.

x	θ			
	0	$\frac{\pi}{4}$	$\frac{\pi}{2}$	π
$x = 0.1$	0.5681	0.7941	3.0724	4.7120
$x = 0.2$	1.7148	7.3121	19.0337	5.5256
$x = 0.3$	12.2184	38.1826	38.1826	3.7062

Table-2. The variation of heat transfer coefficient Z with $\Pr E$ for $\phi_1 = 0.6$, $\phi_2 = 0.9$, $\lambda_1 = 0.3$, $M = 1, Da = 0.1, \theta = \frac{\pi}{4}$ and $d = 2$.

x	$\Pr E$		
	1	2	3
$x = 0.1$	0.6721	0.7331	0.7941
$x = 0.2$	3.2981	5.3051	7.3121
$x = 0.3$	13.9151	26.0489	38.1826

Table-3. The variation of heat transfer coefficient Z with M for $\phi_1 = 0.6$, $\phi_2 = 0.9$, $\lambda_1 = 0.3$, $\Pr E = 2, Da = 0.1, \theta = \frac{\pi}{4}$ and $d = 2$.

x	M		
	0	1	2
$x = 0.1$	0.7294	0.7331	0.7436
$x = 0.2$	5.2074	5.3051	5.5872
$x = 0.3$	25.7210	26.0489	27.1061

Table-4. The variation of heat transfer coefficient Z with Da for $\phi_1 = 0.6$, $\phi_2 = 0.9$, $\lambda_1 = 0.3$, $M = 1, Da = 0.1, \theta = \frac{\pi}{4}$ and $d = 2$.

x	Da			
	0.01	0.1	10	100
$x = 0.1$	0.9089	0.7331	0.6944	0.6944
$x = 0.2$	10.3682	5.3051	4.6215	4.5878
$x = 0.3$	49.8039	26.0489	27.5832	27.0021

Table-5. The variation of heat transfer coefficient Z with ϕ_1 for $\phi_1 = 0.6, \phi_2 = 0.9$, $\lambda_1 = 0.3$, $M = 1, Da = 0.1, \theta = \frac{\pi}{4}$ and $d = 2$.

x	ϕ_1		
	0.3	0.6	0.9
$x = 0.1$	0.5229	0.7331	0.8785
$x = 0.2$	3.1946	5.3051	6.6179
$x = 0.3$	10.6273	26.0489	48.1259

5. CONCLUSIONS

In this paper, we investigated the effects of Heat transfer and MHD on the peristaltic flow of a Jeffrey fluid in asymmetric channel under lubrication approach. The expressions for the velocity filed and temperature field are obtained. It is found that, in the pumping region the time averaged flux $\overline{Q}$ increases with increasing M, ϕ_1 and ϕ_2 while it decrease with increasing θ, λ_1 and d. It is observed that the temperature field Θ increases with increasing Da, ϕ_2, θ and $\Pr E$, while it decreases with increasing M, λ_1, ϕ_1 and d. The heat transfer coefficient Z increases with increasing θ, M, $\Pr E$ and ϕ_1, while it decreases with increasing Da.

ACKNOWLEDGEMENTS

We thank the management of Sri Kalki Supreme Constructions Pvt Ltd Hyderabad, Swamy & Sons Constructions Bangalore, India, for their support, valuable guidelines, consistent encouragement and providing me necessary facilities in pursuing the research work.

Nomenclature

$a_1 + a_2$ width of the channel
b_1, b_2 amplitudes of the lower and upper waves
B_0 uniform magnetic field strength
c speed of the wave/constant speed
d channel width
Da Darcy number
δ the wave number
Δp the dimensionless pressure rise per one wavelength in the wave frame
$\dot{\gamma}$ the shear rate with respect to time t
k thermal conductivity of the fluid
k_0 the permeability of the porous medium
l wavelength
λ_1 ratio of relaxation time to retardation time
l_2 the retardation time
μ the dynamic viscosity /the co- efficient of viscosity of the fluid
M Hartmann number
ϕ_1 amplitude ratio of the upper wave
ϕ_2 amplitude ratio of the lower wave
p pressure in wave frame of reference
P pressure in fixed frame of reference
q volume flow rate in a wave frame
$Q(x, t)$ the flux at any axial station in the laboratory frame
$\overline{Q}$ the time-averaged volume flow rate
$\mathrm{Re} = \frac{\rho a_1 c}{\mu}$ the Reynolds number
ρ the density
σ the electrical conductivity of the fluid
ζ the specific heat at constant volume
θ phase shift / phase difference : $0 \le \theta \le \pi$
T temperature of the fluid.
t stress tensor
v kinematic viscosity of the fluid
(u, v) and (U, V) velocity components in wave and fixed frames
(x, y) moving frame of reference
(X, Y) fixed frame of reference
Z the heat transfer coefficient at the upper wall

REFERENCES

[1] Provost. A. M. and Schwarz. W. H. 1994. A theoretical study of viscous effects in peristaltic pumping. J. Fluid Mech. 279: 177-195.

[2] Hayat. T., Ali. N., Asghar. S. and Siddiqui. A. M. 2006. Exact peristaltic flow in tubes with an endoscope, Appl. Math. Comput. 182: 359-368.

[3] Nagendra. N., Madhava Reddy. N. and Subba Reddy. M.V. and Jayaraj. B. 2008. Peristaltic flow of a Jeffrey fluid in a tube. Journal of Pure and Applied Physics. 20: 189-201.

[4] Mekheimer. Kh. S. and Al-Arabi. T.H. 2003. Nonlinear peristaltic transport of MHD flow through a porous medium. Int. J. Math. Math. Sci. 26: 1663-1682.

[5] Hayat. T. and Ali. N. 2008. Peristaltic motion of a Jeffrey fluid under the effect of a magnetic field in a tube, Communications in Nonlinear Science and Numerical Simulation. 13: 1343-1352.

[6] Hayat. T., Ahamad. N. and Ali N. 2008. Effects of an endoscope and magnetic field on the peristalsis involving Jeffrey fluid, Communications in Nonlinear Science and Numerical Simulation. 13: 1581-1591.

[7] El Shehawey. E.F. and Husseny. S.Z.A. 2000. Effects of porous boundaries on peristaltic transport through a porous medium. Acta Mechanica. 143: 165-177.

[8] El Shehawey. E.F., Mekheimer. Kh. S, Kaldas. S.F and Afifi N. A. S. 1999. Peristaltic transport through a porous medium. J. Biomath. vol. 14.

[9] Hayat. T., Umar Qureshi. M. and Hussain. Q. 2009. Effect of heat transfer on the peristaltic flow of an electrically conducting fluid in a porous space, Applied Mathematical Modelling. 33: 1862-1873.

[10] Sudhakar Reddy. M., Subba Reddy. M.V and Ramakrishna. S. 2009. Peristaltic motion of a carreau fluid through a porous medium in a channel under the effect of a magnetic field. Far East Journal of Applied Mathematics. 35: 141-158.

[11] Mishra. M. and Ramachandra RAO. A. 2003. Peristaltic transport of a Newtonian fluid in an asymmetric channel, Z. Angew. Math. Phys. (ZAMP). 54: 532-550.

[12] Ramachandra Rao. A. and Mishra. M. 2004. Peristaltic transport of a power-law fluid a porous tube. J. Non-Newtonian Fluid Mech. 121: 163-174.

[13] Eytan. O. and Elad. D. 1999. Analysis of Intra - Uterine fluid motion induced by uterine contractions. Bull. Math. Bio. 61: 221-238.

[14] Eytan. O., Jaffa. A.J. and Elad. D. 2001. Peristaltic flow in a tapered channel: application to embryo transport within the uterine cavity, Med. Engng. Phys. 23: 473-482.

[15] EL Shehawey. E.F. Eldabe. N.T. Elghazy. E.M. and Ebaid. A. 2006. Peristaltic transport in an asymmetric channel through a porous medium. Appl. Math. comput. 182: 140-150.

[16] Subba Reddy. M.V. Ramachandra Rao. A. and Sreenadh. S. 2007. Peristaltic motion of a power law fluid in an asymmetric channel. Int. J. Non-Linear Mech. 42: 1153-1161.

[17] Ali. N. and Hayat. T. 2007. Peristaltic motion of a Carreau fluid in an asymmetric channel. Appl. Math. Comput. 194: 535-552.

[18] Mekheimer. Kh. S, Abd elmaboud. Y. 2007. The influence of heat transfer and magnetic field on peristaltic transport of a Newtonian fluid in a vertical annulus: application of an endoscope. Physics A. pp.1-9.

[19] Vajravelu. K, Radhakrishnamacharya. G, Radhakrishnamurty. V. 2007. Peristaltic flow and heat transfer in a vertical porous annulus with long wave approximation. Int J Nonlinear Mech. 42: 754-759.

[20] Radhakrishnamacharya Srinivasulu. Ch. 2007. Influence of wall properties on peristaltic transport with heat transfer. C R Mecanique. 73 : 335-369.

[21] Srinivas. S, Kothandapani. M. 2007. Peristaltic transport in an asymmetric channel with heat transfer, A note. Int. Commun Heat Mass Trans. pp.1-9.